The First One-Dimensional Iron Phosphite−Phosphate, [Fe^{III}(2,2′-bipyridine)(HPO_3)(H_2PO_4)]: Synthesis, Structure, and Magnetic Properties

Sukhendu Mandal,[†] Swapan K. Pati,[‡] Mark A. Green,[§] and Srinivasan Natarajan*,[†]

Framework Solids Laboratory, Solid State and Structural Chemistry Unit, Indian Institute of Science, Bangalore 560 012, India, Theoretical Sciences Unit, Jawaharlal Nehru Centre for Advanced Scientific Research, Jakkur P.O., Bangalore 560 064, India, and Davy-Faraday Research Laboratory, The Royal Institution of Great Britain, 21 Albermarle Street, London WIS 4BS, U.K.

Received June 11, 2004. Revised Manuscript Received September 24, 2004

A hydrothermal reaction of a mixture containing iron powder, phosphorus acid, 2,2′-bipyridine, and water at 125 °C for 7 days gave colorless rods of a new hybrid iron phosphite−phosphate, [Fe^{III}(2,2′-bipyridne)(HPO_3)(H_2PO_4)], **I**. The structure consists of an edge-shared four-membered ring formed by the connectivity between FeO_4N_2 octahedra, pseudo-pyramidal HPO_3 units. 2,2′-Bipyridine and $PO_2(OH)_2$ tetrahedra are grafted onto the Fe center and hang into the interchain spaces. This is the first observation, to our knowledge, of a one-dimensional edge-shared chain structure in iron phosphite/phosphate. The structure appears to have close similarity to an iron arsenate-oxalate, $[C_4N_2H_{12}][Fe(OH)(HAsO_4)(C_2O_4)]\cdot H_2O$, and a cadmium phosphate, [Cd(2,2′-bpy)(H_2PO_4)$_2$. Magnetic investigations reveal that the iron is present in the +3 oxidation state and shows antiferromagnetic interactions with typical low-dimensional behavior. The magnetic interactions between the Fe^{3+} ions are modeled using classical uniform chain solution with a single coupling constant *J*, formulated by Fisher involving nearest and next-nearest neighbor exchange interactions, based on the $S = {}^5/_2$ Heisenberg antiferromagentic chain.

Introduction

Open-framework transition metal phosphates are an important class of compounds investigated in great detail during the past decade or so.[1] The continuing interest is primarily due to the possibility of investigating the interplay of structure, dimensionality, and magnetism in these compounds. Thus, iron phosphates with one-,[2−4] two-,[5−11] and three-dimensionally[12−18] extended structures have been prepared and characterized. Recently, the pseudo-pyramidal phosphite, HPO_3, group has been investigated as a possible replacement for the traditional phosphate tetrahedra with great success. A new series of organic amine incorporated metal phosphites with extended network structures have been prepared. Thus, open-framework phosphites of V,[19−23] Cr,[22−24] Mn,[25] Fe,[23,26] Co,[27] Zn,[28−46] Al,[47] Ga,[48] Be,[49] and

* Corresponding author. E-mail: snatarajan@sscu.iisc.ernet.in.
† Indian Institute of Science.
‡ Jawaharlal Nehru Centre for Advanced Scientific Research.
§ The Royal Institution of Great Britain.

(1) Lii, K. H.; Huang, Y.-F.; Zima, V.; Huang, C.-Y.; Lin, H.-M.; Cheng, J.-C.; Liao, F.-L.; Wang, S.-L. *Chem. Mater.* **1998**, *10*, 2599 and references therein.
(2) Cavellec, M.; Riou, D.; Greneche, J.-M.; Ferey, G. *Inorg. Chem.* **1997**, *36*, 2187.
(3) Zima, V.; Lii, K. H. *J. Chem. Soc., Dalton Trans.* **1998**, 4109.
(4) Lethbridge, D. A. Z.; Lightfoot, P.; Morris, R. E.; Wragg, D. S.; Wright, P. A.; Kvick, Å.; Vaughan, G. *J. Solid State Chem.* **1999**, *142*, 455.
(5) Cavellec, M.; Riou, D.; Ferey, G. *J. Solid State Chem.* **1994**, *112*, 441.
(6) Cavellec, M. R.; Greneche, J. M.; Riou, D.; Ferey, G. *Chem. Mater.* **1998**, *10*, 1914.
(7) DeBord, J. R. D.; Reiff, W. M.; Haushalter, R. C.; Zubieta, J. *J. Solid State Chem.* **1996**, *125*, 186.
(8) Lii, K.-H.; Haung, Y.-F. *Chem. Commun.* **1997**, 1311.
(9) Zima, V.; Lii, K.-H.; Nguyen, N.; Ducouret, A. *Chem. Mater.* **1998**, *10*, 1914.
(10) Mgaidi, A.; Boughzala, H.; Driss, A.; Clerac, R.; Coulon, C. *J. Solid State Chem.* **1999**, *144*, 163.
(11) Cowley, A. R.; Chippendale, A. M. *J. Chem. Soc., Dalton Trans.* **2000**, 3425.
(12) Choudhury, A.; Natarajan, S.; Rao, C. N. R. *Chem. Commun.* **1999**, 1305.
(13) Cavellec, M.; Riou, D.; Ferey, G. *Inorg. Chim. Acta* **1999**, *291*, 317.
(14) Cavellec, M.; Riou, D.; Grenenche, J.-M.; Ferey, G. *J. Magn. Magn. Mater.* **1996**, *163*, 173.
(15) Cavellec, M.; Eagger, C.; Linares, L.; Nogues, M.; Varret, F.; Ferey, G. *J. Solid State Chem.* **1997**, *134*, 349.
(16) Lii, K.-H.; Huang, Y.-F. *Chem. Commun.* **1997**, 839.
(17) Lii, K.-H.; Huang, Y.-F. *J. Chem. Soc., Dalton Trans.* **1997**, 2221.
(18) Debord, J. R. D.; Reiff, W. M.; Warren, C. J.; Haushalter, R. C.; Zubieta, J. *Chem. Mater.* **1997**, *9*, 1994.
(19) Shi, Z.; Zhang, D.; Li, G. H.; Wang, L.; Lu, X. Y.; Hua, J.; Feng, S. H. *J. Solid State Chem.* **2003**, *172*, 464.
(20) Harrison, W. T. A. *Solid State Sci.* **2003**, *5*, 297.
(21) Shi, Z.; Li, G. H.; Zhang, D.; Hua, J.; Feng, S. H. *Inorg. Chem.* **2003**, *42*, 2357.
(22) Fernandez, S.; Mesa, J. L.; Pizarro, J. L.; Lezama, L.; Arriortua, M. I.; Rojo, T. *Chem. Mater.* **2003**, *15*, 1204.
(23) Fernandez, S.; Mesa, J. L.; Pizarro, J. L.; Lezama, L.; Arriortua, M. I.; Rojo, T. *Chem. Mater.* **2002**, *14*, 2300.
(24) Fernandez, S.; Mesa, J. L.; Pizarro, J. L.; Lezama, L.; Arriortua, M. I.; Rojo, T. *Angew. Chem., Int. Ed.* **2002**, *41*, 3683.
(25) Fernandez, S.; Mesa, J. L.; Pizarro, J. L.; Lezama, L.; Arriortua, M. I.; Olazcuaga, R.; Rojo, T. *Chem. Mater.* **2000**, *12*, 2092.
(26) Fernandez-Armas, S.; Mesa, J. L.; Pizarro, J. L.; Garitaonandia, J. S.; Arriortua, M. I.; Rojo, T. *Angew. Chem., Int. Ed.* **2004**, *43*, 977.
(27) Fernandez, S.; Mesa, J. L.; Pizarro, J. L.; Lezama, L.; Arriortua, M. I.; Rojo, T. *Int. J. Inorg. Mater.* **2001**, *3*, 331.
(28) Fu, W. S.; Shi, Z.; Li, G. N.; Zhang, D.; Dong, W. J.; Chen, X. B.; Feng, S. H. *Solid State Sci.* **2004**, *6*, 225.
(29) Gorden, L. E.; Harrison, W. T. A. *Inorg. Chem.* **2004**, *43*, 1808.
(30) Lin, Z. E.; Zhang, M.; Zheng, S. T.; Yang, G. Y. *Eur. J. Inorg. Chem.* **2004**, 953.
(31) Fu, W. S.; Wang, L.; Shi, Z.; Li, G. H.; Chen, X. B.; Dai, Z. M.; Yang, L.; Feng, S. H. *Cryst. Growth Des.* **2004**, *4*, 297.

10.1021/cm049064p CCC: $30.25
Published on Web 01/13/2005

Mo[50] have been synthesized and characterized. Although the synthesis of phosphite framework has been accomplished, the investigations on mixed ligands are rare. As far as we are aware, there have been only three previous reports incorporating both the pseudo-pyramidal phosphite, $[HPO_3]^{2-}$, and the tetrahedral phosphate $[PO_4]^{3-}$ oxoanions as part of the inorganic skeleton.[26,46,47] We have been investigating the formation of novel iron phosphites in the presence of organic amine molecules employing hydrothermal methods. During the course of these investigations, we have now isolated a new iron phosphite−phosphate, $[Fe^{III}(C_{10}N_2H_8)(HPO_3)(H_2PO_4)]$, **I**, possessing one-dimensional structure. To our knowledge, this is the first report of a one-dimensional edge-shared chain structure in an iron phosphite/phosphate system. In this paper, we describe the synthesis, structure, and magnetic behavior of this compound.

Experimental Section

Synthesis and Initial Characterization. The iron phosphite−phosphate, $[Fe^{III}(C_{10}N_2H_8)(HPO_3)(H_2PO_4)]$, **I**, was synthesized under hydrothermal conditions using iron metal powder as the source of iron. In a typical synthesis, 0.108 g of Fe-powder was dispersed in 7 mL of deionized water. To this was added 0.636 g of H_3PO_3. Finally, 0.909 g of 2,2′-bipyridine (2,2′-bpy) was added to the mixture and homogenized for 30 min at room temperature. The final mixture with the composition $1.0Fe:4.0H_3PO_3:3.0(2,2'\text{-bpy}):200H_2O$ was transferred into a 23-mL acid-digestion bomb and heated at 125 °C for 7days. The resulting product, containing large quantities of colorless rodlike single crystals, was filtered, washed with deionized water, and dried at ambient conditions. The yield of the product was ∼70% based on Fe. The initial and final pH of the reaction mixture was ∼2.

The initial characterization was carried out using powder X-ray diffraction (XRD), thermogravimetric analysis (TGA), and infrared (IR) measurements. An EDAX analysis on the single crystal indicated an Fe:P ratio of 1:2, consistent with the single-crystal data. The powder XRD patterns were recorded on crushed single crystals in the 2θ range 5−30° using Cu Kα radiation (Rich-Seifert, 3000TT). The XRD pattern was entirely consistent with the structures determined using the single-crystal X-ray diffraction.

Thermogravimetric analysis (TGA) has been carried out (Mettler-Toledo, TG850) in nitrogen atmosphere (flow rate = 50 mL/min) in the temperature range 25−800 °C (heating rate = 5 °C/min^{-1}). The studies show broad weight losses in three overlapping steps, which begin gradually at 250 °C and are complete at 700 °C. The total weight loss of 42.6% corresponds to the loss of the bonded amine molecule and the condensation of the terminal hydroxyl group of the H_2PO_4 units (calc. = 44.9%). The calcined sample was amorphous to powder XRD.

Infrared (IR) spectroscopic studies carried out in the range 400−4000 cm^{-1} using the KBr pellet method (Bruker IFS-66v) exhibited typical peaks corresponding to the 2,2′-bpy, H_2PO_4, and HPO_3 moieties. IR bands: ν(NH) = 3037 cm^{-1}, ν(CH) = 3110 cm^{-1}, ν(PH) = 2388 cm^{-1}, δ(NH) = 1598 cm^{-1}, δ(CH) = 1476 cm^{-1}, δ(HP) = 940 cm^{-1}, δs (PO_3) = 599 cm^{-1}, δas (PO_3) = 542 cm^{-1}.

The temperature variation of the magnetic susceptibility studies has been carried out on powdered single crystals in the range 2−300 K with a SQUID magnetometer (Quantum Design MPMS7 SQUID). Measurements were carried out when the sample had been through both a zero-field cooled and a field-cooled procedure.

Single-Crystal Structure Determination. A suitable colorless single crystal was carefully selected under a polarizing microscope and glued to a thin glass fiber with cyanoacrylate (superglue) adhesive. Crystal structure determination by X-ray diffraction was performed on Siemens SMART − CCD diffractometer equipped with a normal focus, 2.4 kW sealed tube X-ray source (Mo Kα radiation, λ = 0.71073 Å) operating at 40 kV and 40 mA. A hemisphere of intensity data was collected at room temperature in 1321 frames with ω scans (width of 0.30° and exposure time of 10 s per frame) in the 2θ range 3−46.5°. Pertinent experimental details for the structure determination of **I** are presented in Table 1.

An empirical absorption correction was applied using the SADABS program.[51] The structure was solved and refined using the SHELXL suit of programs.[52] The direct method solution readily

Table 1. Crystal Data and Structure Refinement Parameters for $[Fe^{III}(C_{10}N_2H_8)(HPO_3)(H_2PO_4)]$, I

empirical formula	$Fe_1P_2O_7C_{10}N_2H_{11}$
formula weight	392.03
crystal system	monoclinic
space group	$P2_1/m$ (No. 11)
a (Å)	10.541(1)
b (Å)	6.430(1)
c (Å)	10.617 (1)
β (deg)	113.89 (1)
volume (Å^3)	657.93 (3)
Z	4
T (K)	293(2)
ρ_{calc} (g cm^{-3})	1.878
μ (mm^{-1})	1.418
θ range (deg)	2.10−23.25°
λ (Mo Kα) (Å)	0.71073
R indexes [$I > 2\sigma(I)$]	$R_1 = 0.0385$, w$R_2 = 0.0944$[a]
R (all data)	$R_1 = 0.0495$, w$R_2 = 0.101$

[a] $R_1 = \sum||F_o| - |F_c||/\sum|F_o|$; w$R_2 = \{\sum[w(F_o^2 - F_c^2)^2]/\sum[w(F_o^2)^2]\}^{1/2}$; $w = 1/[\sigma^2(F_o)^2 + (aP)^2 + bP]$, $P = [\max.(F_o^2,0) + 2(F_c)^2]/3$, where a = 0.0460 and b = 1.5472.

(32) Lin, Z. E.; Zhang, J.; Zheng, S. T.; Yang, G. Y. *Microporous Mesoporous Mater*. **2004**, *68*, 65.
(33) Shi, S. H.; Li, G. H.; Xin, H. M.; Ding, H.; Xu, J. N.; Zhu, G. S.; Song, T. Y.; Qiu, S. J. *Chem. J. Chin. Univ.* **2004**, *25*, 230.
(34) Wang, L.; Shi, Z.; Fu, W. S.; Li, G. H.; Zhang, D.; Dong, W. J.; Dai, Z. M.; Chen, X. B.; Feng, S. H. *J. Solid State Chem*. **2004**, *177*, 80.
(35) Zhang, D.; Shi, Z.; Dong, W.; Fu, W. S.; Wang, L.; Li, G. H.; Feng, S. H. *J. Solid State Chem*. **2004**, *177*, 343.
(36) Lin, Z. E.; Zhang, J.; Zheng, S. T.; Wei, Q. H.; Yang, G. Y. *Solid State Sci*. **2003**, *5*, 1435.
(37) Dong, W. J.; Li, G. H.; Shi, Z.; Fu, W. S.; Zhang, D.; Chen, X. B.; Dai, Z. M.; Wang, L.; Feng, S. H. *Inorg. Chem. Commun*. **2003**, *6*, 776.
(38) Wang, Y.; Yu, J. H.; Li, Y.; Du, Y.; Xu, R. R.; Ye, L. *J. Solid State Chem*. **2003**, *170*, 303.
(39) Liang, J.; Wang, Y.; Yu, J. H.; Li, Y.; Xu, R. R. *Chem. Commun*. **2003**, 882.
(40) Harrison, W. T. A.; Phillips, M. L. F.; Stranchfield, J.; Nenoff, T. M. *Inorg. Chem*. **2001**, *40*, 895.
(41) Harrison, W. T. A. *Int. J. Inorg. Mater*. **2001**, *3*, 187.
(42) Harrison, W. T. A. *J. Solid State Chem*. **2001**, *160*, 4.
(43) Harrison, W. T. A.; Phillips, M. L. F.; Nenoff, T. M. *Int. J. Inorg. Mater*. **2001**, *3*, 1033.
(44) Harrison, W. T. A.; Phillips, M. L. F.; Nenoff, T. M. *J. Chem. Soc., Dalton Trans*. **2001**, 2459.
(45) Rodgers, J. A.; Harrison, W. T. A. *Chem. Commun*. **2000**, 2385.
(46) Wang, Y.; Yu, J. H.; Du, Y.; Shi, Z.; Zou, Y. C.; Xu, R. R. *J. Chem. Soc., Dalton Trans*. **2002**, 4060.
(47) Harvey, H. G.; Hu, J.; Attfield, M. P. *Chem. Mater*. **2003**, *15*, 179.
(48) Fernandez-Armes, S.; Mesa, J. L.; Pizarro, J. L.; Lezama, L.; Arriortua, M. I.; Rojo, T. *J. Solid State Chem*. **2004**, *177*, 765.
(49) Fu, W. S.; Wang, L.; Shi, Z.; Li, G. H.; Chen, X. B.; Dai, Z. M.; Yang, L.; Feng, S. H. *Cryst. Growth Des.* **2004**, *4*, 297.
(50) Lyxell, D. G.; Bostrom, D.; Hashimoto, M.; Petterson, L. *Acta Chem. Scand.* **1998**, *52*, 425.
(51) Sheldrick, G. M. *SADABS Siemens Area Correction Absorption Correction Program*; University of Göttingen, Göttingen, Germany, 1994.
(52) Sheldrick, G. M. *SHELXL-97 Program for Crystal Structure Solution and Refinement*; University of Göttingen, Göttingen, Germany, 1997.

Table 2. Selected Bond Distances and Angles in $[Fe^{III}(2,2'\text{-bpy})(HPO_3)(H_2PO_4)]$, I[a]

bond	distance (Å)	bond	distance (Å)
Fe(1)−O(1)	1.919(4)	P(1)−O(3)	1.505(3)
Fe(1)−O(2)	1.938(4)	P(1)−O(3)#2	1.505(3)
Fe(1)−O(3)	1.989(3)	P(1)−O(2)#3	1.511(4)
Fe(1)−O(3)#1	1.989(3)	P(2)−O(1)	1.479(5)
Fe(1)−N(1)	2.177(5)	P(2)−O(4)	1.510(5)
Fe(1)−N(2)	2.178(5)	P(2)−O(5)	1.577 (4)
		P(2)−O(5)#1	1.577 (4)

moiety	angle (deg)	moiety	angle (deg)
O(1)−Fe(1)−O(2)	102.2(2)	O(1)−Fe(1)−O(3)#1	92.52(10)
O(2)−Fe(1)−O(3)#1	93.60(8)	O(1)−Fe(1)−O(3)	92.52(10)
O(2)−Fe(1)−O(3)	93.60(9)	O(3)#1−Fe(1)−O(3)	170.1(2)
O(1)−Fe(1)−N(1)	91.8(2)	O(2)−Fe(1)−N(1)	166.0(2)
O(3)#1−Fe(1)−N(1)	85.69(8)	O(3)−Fe(1)−N(1)	85.69(8)
O(1)−Fe(1)−N(2)	166.4(2)	O−(2)−Fe(1)−N(2)	91.3(2)
O(3)#1−Fe(1)−N(2)	86.56(10)	O(3)−Fe(1)−N(2)	86.55(10)
N(1)−Fe(1)−N(2)	74.6(2)	O(3)#2−P(1)−O(3)	110.1(2)
O(3)#2−P(1)−O(2)#3	114.0(2)	O(3)−P(1)−O(2)#3	114.0(2)
O(1)−P(2)−O(4)	111.8(3)	O(1)−P(2)−O(5)	109.8(3)
O(4)−P(2)−O(5)	114.3(3)	O(1)−P(2)−O(5)#1	109.8(3)
O(4)−P(2)−O(5)#1	114.3(3)	O(5)−P(2)−O(5)#1	95.8(6)
P(2)−O(1)−Fe(1)	172.1(3)	P(1)#3−O(2)−Fe(1)	138.5(3)
P(1)−O(3)−Fe(1)	141.5(2)	C(5)−N(1)−Fe(1)	117.6(4)
C(1)−N(1)−Fe(1)	124.4(4)	C(10)−N(2)−Fe(1)	124.2(4)

[a] Symmetry transformation used to generate equivalent atoms: #1, x, $-y + {}^1/_2$, z; #2, x, $-y - {}^1/_2$, z; #3, $-x$, $-y$, $-z + 1$.

revealed sufficient fragments of the structure (Fe, P, and O) and enabled the remainder of the non-hydrogen atoms to be located from difference Fourier maps and the refinements to proceed to $R < 10\%$. The hydrogen atom in the P−H group and all other hydrogen positions were initially located in the difference Fourier map, and for the final refinement the hydrogen atoms were placed in geometrically ideal positions and refined using the riding mode. The last cycles of refinements included atomic positions, anisotropic thermal parameters for all of the non-hydrogen atoms, and isotropic thermal parameters for all of the hydrogen atoms. Full-matrix-least-squares structure refinement against $|F|^2$ was carried out using the SHELXL package of programs.[52] Selected bond distances and angles for **I** are presented in Table 2.

Results and Discussion

The asymmetric unit of **I** contains 19 non-hydrogen atoms, of which one iron and two phosphorus atoms are crystallographically independent (Figure 1). Except for one oxygen atom, O(3), all of the other atoms in the asymmetric unit are situated in the mirror plane. The iron atom is octahedrally coordinated by two nitrogen atoms of the 2,2′-bpy ligand and four oxygen atoms. The Fe−O bond averages a distance of 1.959 Å, and the Fe−N bonds average 2.177 Å. The iron atom is connected to two distinct phosphorus atoms through Fe−O−P bonds. The two P atoms, P(1) and P(2), have pseudo-tetrahedral and tetrahedral connectivity with respect to the oxygen atoms. While P(1) is connected to iron through three P−O−Fe bonds and possesses the terminal P−H bond, P(2) is connected by two P−O−Fe bonds and possesses two terminal P−O bonds. The P−O bonds average a distance of 1.499 Å to the oxygen atoms without bonded hydrogen atoms, and 1.577 Å to oxygens bonded to hydrogen atoms.

The structure of **I** consists of a network of octahedral FeO_4N_2 and pseudo-tetrahedral $HP(1)O_3$ units, strictly alternating, connected through their vertices to give rise to a four-membered ring. The four-membered rings are connected edge-wise to form a one-dimensional chain structure. The $P(2)O_2(OH)_2$ tetrahedra and 2,2′-bipyridine molecules are grafted onto this one-dimensional structure by bonding with the iron center (Figure 2). Looking down the one-dimensional structure, one can see that the 2,2′-bipyridine molecules do not lie exactly one over the other, but are slightly shifted. The 2,2′-bipyridine ligands from two different one-dimensional chains, projecting into the interchain spaces, are separated by ∼7 Å, indicating little interactions between them. The hanging $PO_2(OH)_2$ with the two terminal P−(OH) bonds, on the other hand, can be potential donor and acceptor groups and interacts through O−H···O hydrogen bonds (O−O contact distance = 2.78 Å). Thus, the one-dimensional

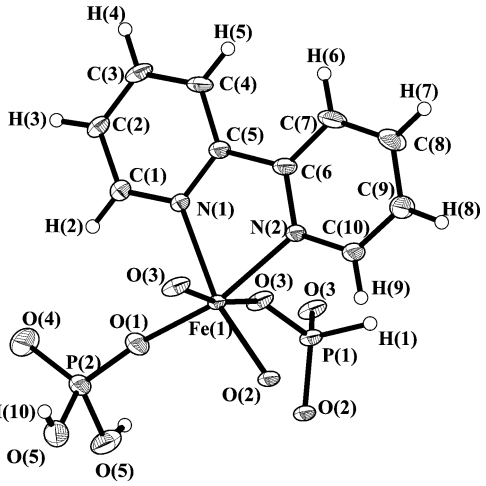

Figure 1. ORTEP plot of **I**, showing the asymmetric unit. Thermal ellipsoids are given at 50% probability.

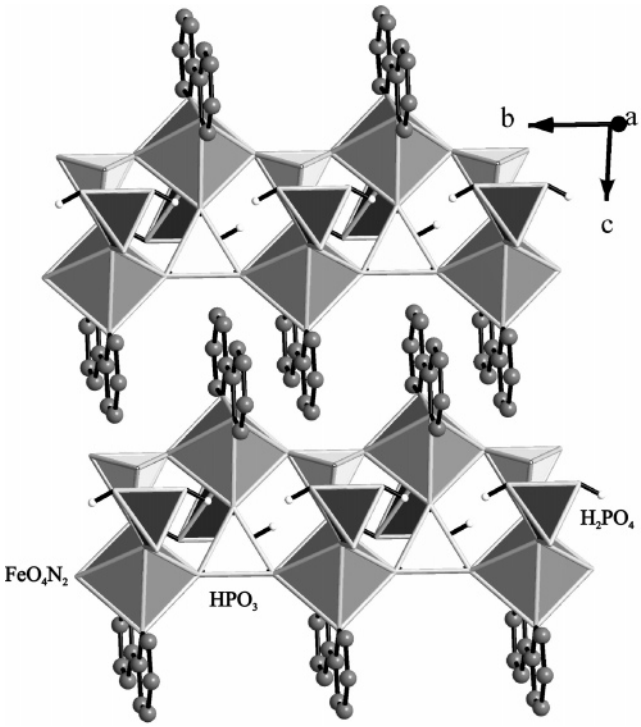

Figure 2. Polyhedral view of the structure of **I** in the *bc* plane showing the arrangement of the one-dimensional edge-shared chains. Hydrogen atoms on the 2,2′-bpy molecules are not shown for clarity.

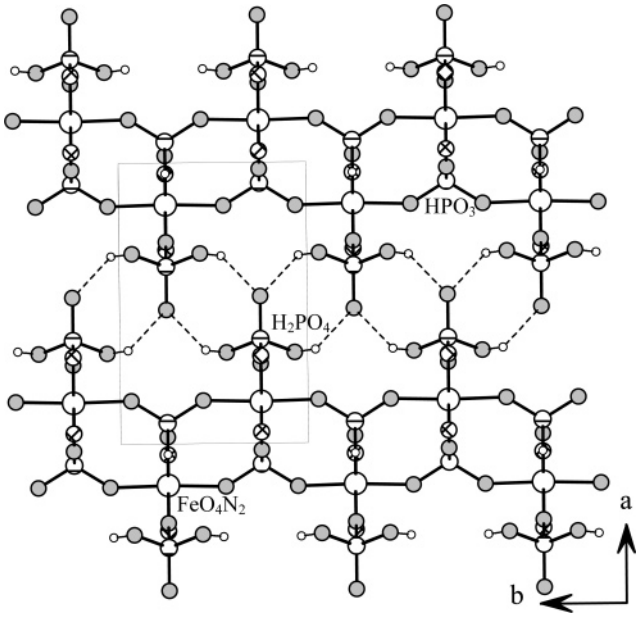

Figure 3. Structure of **I** in the *ab* plane showing the one-dimensional chains. The 2,2′-bpy molecules are not shown for clarity. The dotted lines represent possible hydrogen-bond interactions. Note that the hydrogen-bond interactions between the hanging $PO_2(OH)_2$ tetrahedra create a layerlike structure.

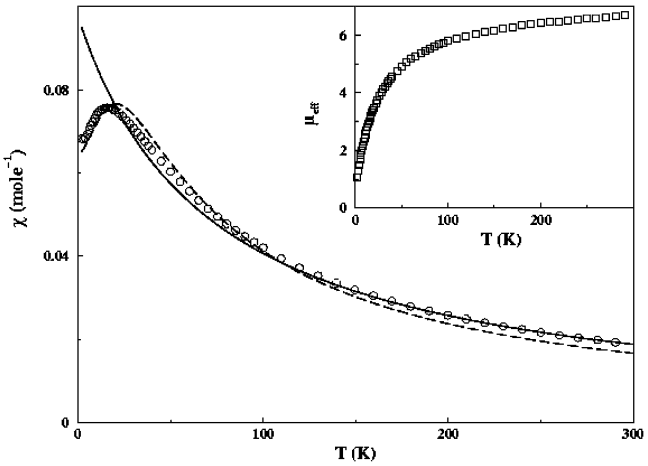

Figure 4. Temperature variation of the magnetic susceptibility of **I**. Curie−Weiss fit (solid line) and Fisher's formula fit (classical $S = {}^5/_2$ Heisenberg moments, dashed line) (see text). The inset shows the temperature variation of the magnetic moment (μ_{eff}).

chains are supramolecularly linked through the hydrogen bonds forming a two-dimensional layer as shown in Figure 3.

The magnetic investigations show that **I** orders antiferromagnetically (AFM) at low temperatures. The temperature variation of the magnetic susceptibility is given in Figure 4. It is quite clear that the system shows a broad maximum around $T = 20$ K, below which the susceptibility drops quite sharply. At high temperatures, the susceptibility value saturates to the paramagnetic spin-only value of an Fe^{3+} spin ($5.91\mu_B$). The observed μ_{eff} is within the range expected for high-spin Fe^{3+} compounds and corresponds well with the spin-only value (5.92 μ_B; typical values 5.65−6.10 μ_B[53]). The high-temperature magnetic susceptibility exhibits a behavior, which can be approximated by a Curie−Weiss law (solid line in Figure 4). The fit of the susceptibility to a form $\chi = (C/T - \theta)$ in the temperature range 100−300 K gives a value of 7.0 and 69 K for C and θ, respectively.

Scheme 1

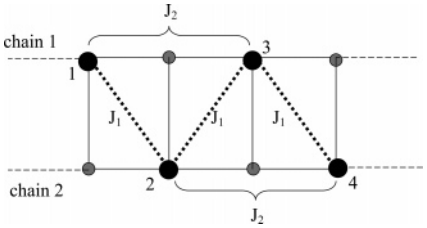

In **I**, the broad maximum of $\chi(T)$ at 20(1) K indicates low-dimensional antiferromagnetic interactions.[54] The Fe^{3+}-ions (classical $S = {}^5/_2$ Heisenberg moments) form a zigzag chain with two kinds of O−P−O bridges, one within a chain with coupling J_a and another between the Fe-species of the neighboring independent chain with coupling J_b (Figure 3). This geometrical arrangement of Fe^{3+} ions can lead to spin frustration for negative J_a and J_b of similar magnitudes. In a preliminary model, for $|J_a| \gg |J_b|$, this spin-frustrated chains can be approximated by the classical uniform chain solution with coupling J, formulated by Fisher.[55] For a classical Heisenberg linear periodic chain with the spin vector of magnitude $[S(S + 1)]^{1/2}$, the Fisher's zero-field magnetic susceptibility is given by the equation:

$$\chi/N = [g^2S(S + 1)\mu_B{}^2/3k_BT][(1 + u)/(1 - u)]$$

where

$$u = \coth[2JS(S + 1)/k_BT] - k_BT/[2JS(S + 1)]$$

The leading terms in the high-temperature expansion of this equation agree quite well with those derived by Rushbrooke and Wood,[56] for a linear Heisenberg chain model. This model has been successfully employed to explain the antiferromagnetic behavior of $CsMnCl_3{\cdot}2H_2O$.[57,58] This form of the susceptibility is common to infinite one-dimensional chain with an exponentially decaying correlation function $[\langle S_oS_r\rangle \approx \exp(-r/\xi)]$, where the correlation length (ξ) and the parameter u are related by the expression, $|u| = \exp(-1/\xi)$. Assuming $S = {}^5/_2$ and $g = 2$, we have fitted the above equation with our data by adjusting the single coupling constant, J (dashed line in Figure 4). The fitting gave rise to a value of $J = -4.42$ K. Because J is antiferromagnetic, the susceptibility exhibits a rounded maximum and approaches a finite value of ~0.61 as $T \rightarrow 0$. It may be noted that this value of J nicely mimics the temperature and shape of the maximum in the $\chi-T$ curve.

To understand the frustration in such a quasi one-dimensional system as shown in Scheme 1 above and also to evaluate the strength of the interactions, we have made a careful investigation of the exchange pathways within the

(53) König, E.; König, G. *Landolt-Börnstein, New Series*; Springer: Berlin, 1984; Vol. 12/4a.
(54) Hatfield, W. E.; Estes, W. E.; Marsh, W. E.; Pickens, M. W.; ter Haar, L. W.; Weller, R. R. In *Extended Linear Chain Compounds*; Miller, J. S., Ed.; Plenum: New York, 1983; Vol. 3.
(55) Fisher, M. E. *Am. J. Physiol.* **1964**, *32*, 343.
(56) Rushbrook, G. S.; Wood, P. J. *Mol. Phys.* **1958**, *1*, 257.
(57) Schriempf, J. T.; Friedberg, S. A. *J. Chem. Phys.* **1964**, *40*, 296.
(58) Smith, T.; Friendberg, S. A. *Phys. Rev.* **1968**, *176*, 660.

system. The exchange interactions between the Fe^{3+}centers are not linear but are zigzag with nearest and next-neighbor exchange couplings (J_1 and J_2). The preliminary model gave an idea of the system with a single exchange constant, *J*. From the structural point of view, there appears to be two direct possible exchange pathways within the chain as shown in Scheme 1, but both are through the phosphite groups with the distances involved being different. This situation gives rise to two parallel chains of Fe^{3+} ions that are offset by half a unit cell along the chain axis. Thus, an Fe^{3+} ion in one chain is identically connected to two Fe^{3+} ions in the neighboring chain (shown by the dotted line in Scheme 1). This gives rise to two types of interactions. The next-neighbor superexchanges then correspond to the exchanges between these two chains (J_2) of Fe^{3+} ions, the physical superexchange distance of which is almost 1.5 times the nearest-neighbor diagonal superexchange distance (J_1). Interestingly, a model of such a lattice structure is quite well studied in the literature.[59,60] Because obtaining two independent coupling constants is quite difficult, the fitting in Figure 4 was carried out with classical spin limits with a single exchange parameter. We have performed long-chain calculations using quantum many body nonpertabative method (DMRG, density matrix renormalization group)[61,62] of quantum spin-$^5/_2$ chains with nearest and next-neighbor interactions (Scheme 1), with one parameter (α), the ratio of the two exchange constants ($\alpha = J_2/J_1$). Note that a quantum spin-$^5/_2$ zigzag chain with only nearest-neighbor coupling has a gapless spectrum. It is the next-nearest neighbor coupling that introduces frustration and thereby spontaneously dimerizes this system. It is this frustration-induced dimerization that causes the correlation function of the system to decay exponentially (given above). Keeping the nearest-neighbor exchange at unity, we find that the next-nearest neighbor coupling is then approximately 0.4. This naively explains the strength of frustration in this system.

One of the most striking aspects of **I** is the presence of the one-dimensional edge-shared four-membered rings. Although one-dimensional iron phosphates have been prepared and characterized,[2−4] to our knowledge, this is the first report of the chain structure. Most of the one-dimensional iron phosphates tend to form with the tancoite structure, $M\varphi(TO_4)_2$ (M is an octahedrally coordinated element, T is a tetrahedrally coordinated element, and φ is an anionic ligand; e.g., O^{2-}, OH^-, F^-, etc.).[63] The lack of one-dimensional iron phosphates may be explained using the bond valence theory. For the tetrahedral P^{5+}, every oxide ligand receives a bond valence contribution of 1.25 valence units (v.u.), and the remaining 0.75 v.u. for change balancing criterion needs to be supplied by the Fe in the structure. This creates a situation

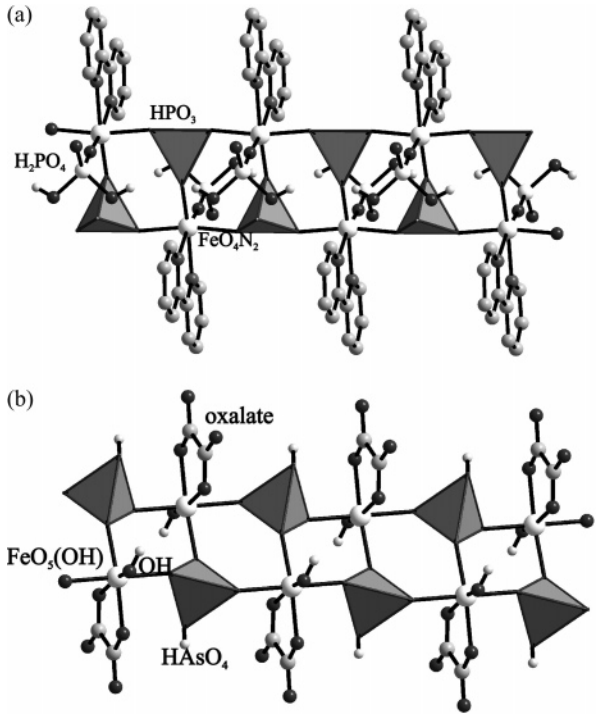

Figure 5. (a) View of a single chain in **I**, $[Fe^{III}(2,2'\text{-bpy})(HPO_3)(H_2PO_4)]$. (b) View of a single chain in the iron arsenate-oxalate, $[C_4N_2H_{12}][Fe(OH)(HAsO_4)(C_2O_4)]\cdot H_2O$. Note the close similarity between the two structures (see text).

wherein the final structures are highly polymerized resulting in extended networks (3D) or sheets (2D), irrespective of other variables that may influence the stoichiometry and structure. In the present case, the use of P^{3+} might have facilitated the formation of this unusual one-dimensional structure.

Of the many transition element phosphates, a one-dimensional cobalt phosphate, $[NH_3(CH_2)_3NH_3][Co(HPO_4)_2]$, with an edge-shared four-membered ring structure has been reported.[64] The cobalt atoms are in tetrahedral coordination, and in a sense they are similar to the many one-dimensional aluminum phosphate edge-shared four-membered ring structures reported in the literature.[65] Yet the structure of the present compound appears to have some relationship to the iron arsenate-oxalate structure, $[C_4N_2H_{12}][Fe(OH)(HAsO_4)(C_2O_4)]\cdot H_2O$, reported recently.[66] In the iron arsenate-oxalate structure, the strictly alternating $FeO_5(OH)$ octahedral and $AsO_3(OH)$ tetrahedral are linked to give rise to edge-shared one-dimensional chains. The −OH and the oxalate groups hang as pendant from the iron center. In **I**, we have FeO_4N_2 octahedra and HPO_3 units linked to form the one-dimensional chain with the 2,2′-bpy and $PO_2(OH)_2$ molecules replacing the oxalate and the −OH group (Figure 5). The present structure is also similar to the recently reported cadmium phosphate, $[Cd(2,2'\text{-bpy})(H_2PO_4)_2]$.[67] In the cadmium phosphate structure, CdO_4N_2 octahedra and $PO_2(OH)_2$ tetrahedra strictly alternate and form edge-shared one-dimensional

(59) Chitra, R.; Pati, S. K.; Krishnamurthy, H. R.; Sen, D.; Ramasesha, S. *Phys. Rev.* **1995**, *B52*, 6581.
(60) Pati, S. K.; Chitra, R.; Sen, D.; Krishnamurthy, H. R.; Ramasesha, S. *Europhys. Lett.* **1996**, *33*, 707.
(61) Pati, S. K.; Chitra, R.; Sen, D.; Ramasesha, S.; Krishnamurthy, H. R. *J. Phys.: Condens. Matter* **1997**, *9*, 219.
(62) Pati, S. K.; Ramasesha, S.; Sen, D. In *Magnetism: Molecules to Materials IV*; Miller, J. S., Drillon, M., Eds.; Wiley−VCH: Weinheim, 2003; p 119.
(63) Ramik, R. A.; Sturman, B. D.; Dunn, P. J.; Poverennykh, A. S. *Can. Mineral.* **1980**, *18*, 185.
(64) Cowley, A. R.; Chippindale, A. M. *J. Chem. Soc., Dalton Trans.* **1999**, 2147.
(65) Yu, J.; Xu, R. R. *Acc. Chem. Res.* **2003**, *36*, 481.
(66) Chakrabarty, S.; Natarajan, S. *Angew. Chem., Int. Ed.* **2002**, *41*, 1224.
(67) Lin, Z. E.; Sun, Y. Q.; Zhang, J.; Wei, Q. H.; Yang, G. Y. *J. Mater. Chem.* **2003**, *13*, 447.

chains. The 2,2′-bpy molecule and $PO_2(OH)_2$ units hang from the Cd center, just like in **I**.

The hydrothermal synthesis offers a convenient method for the preparation of organic−inorganic hybrid compounds. The uniqueness of the organic and inorganic components may be complemented with each other in such materials to give rise to new solid-state structures and in some cases composite structures. In **I**, the use of 2′2-bpy molecule as the ligand creates a situation wherein the traditionally octahedral iron centers bond with P to create a one-dimensional edge-shared chain structure. The partial oxidation of P^{3+} to P^{5+}, in **I**, is unexpected and may be due to the high acidity of the reaction mixture, and such instances have been noted before.[26,46] It is likely that the combination of low temperature and the use of polyfunctional aromatic molecules might give rise to many new solids with novel structures. We are currently pursuing this theme vigorously.

Acknowledgment. S.M. gratefully acknowledges the financial support from the University Grant Commission (UGC), Government of India, through the award of a research fellowship. S.N. thanks the Department of Science and Technology (DST), Government of India, for the award of a research grant. We also thank the reviewers for their helpful suggestions.

Supporting Information Available: Crystallographic information (CIF). This material is available free of charge via the Internet at http://pubs.acs.org.

CM049064P